HHS Public Access

Author manuscript

J Immunol. Author manuscript; available in PMC 2023 January 15.

Published in final edited form as:

J Immunol. 2022 January 15; 208(2): 328–337. doi:10.4049/jimmunol.2100514.

ABCB10 Loss Reduces CD4+ T Cell Activation and Memory Formation

Wenxiang Sun[*,†], **Xuan Jia**[*], **Marc Liesa**[‡], **Dean Tantin**[*,†], **Diane M. Ward**[*,¶]

[*]Department of Pathology, University of Utah, School of Medicine, Salt Lake City UT 84112 USA

[†]Huntsman Cancer Institute, University of Utah, School of Medicine, Salt Lake City UT 84112 USA

[‡]Department of Medicine, Division of Endocrinology, University of California Los Angeles, Los Angeles, CA 90095 USA

Abstract

T cells must shift their metabolism to respond to infections and tumors, and to undergo memory formation. The ATP-binding cassette transporter ABCB10 localizes to the mitochondrial inner membrane, where it is thought to export a substrate important in heme biosynthesis and metabolism, but its role in T cell development and activation is unknown. Here, we use a combination of methods to study the effect of ABCB10 loss in primary and malignantly transformed T cells. Although *Abcb10* is dispensable for development of both $CD4^+$ and $CD8^+$ T cells, it is required for expression of specific cytokines in $CD4^+$ but not $CD8^+$ T cells activated in vitro. These defects in cytokine expression are magnified upon repeated stimulation. In vivo, $CD8^+$ cells lacking ABCB10 expand more in response to viral infection than their control counterparts, while $CD4^+$ cells show reductions both in number and percentage. $CD4^+$ cells lacking ABCB10 show impairment in antigen-specific memory formation and recall responses that become more severe with time. In malignant human $CD4^+$ Jurkat T cells, we find that CRISPR-mediated *ABCB10* disruption recapitulates the same cytokine expression defects upon activation as observed in primary mouse T cells. Mechanistically, *ABCB10* deletion in Jurkat T cells disrupts the ability to switch to aerobic glycolysis upon activation. Cumulatively, these results show that ABCB10 is selectively required for specific cytokine responses and memory formation in $CD4^+$ T cells, suggesting that targeting this molecule could be used to mitigate aberrant T cell activation.

Introduction

T cells require significant metabolic remodeling during activation, proliferation and differentiation. Mitochondria play a key role both in actuating and sensing these changes via their role in synthesizing and transporting metabolites. Quiescent T cells predominantly use mitochondrial oxidative phosphorylation (OXPHOS) to supply their energetic demand. Upon activation, T cells shift their metabolism from OXPHOS to increase glycolysis. The increased glycolytic flux supports cell growth and proliferation as well as T cell lineage

[¶]corresponding author: Diane M. Ward: diane.mcveyward@path.utah.edu, Ph# 801-581-4967, FAX# 801-581-6001.

commitment (1). At the end of the immune response, many responding T cells undergo apoptosis, but a small subset shift metabolism back to a poised/quiescent state and survive as long-lived memory T cells.

The metabolic shifts that occur upon T cell activation increase nutrient consumption. These nutrients need to be either taken up from exogenous sources or synthesized intracellularly. Nutrient transport into cells and transport into and out of the mitochondria has been shown to affect these processes (2–5). Several mitochondrial membrane transporters have been identified that are involved in metabolite import and export. ABCB10 is a mitochondrial ATP-binding cassette (ABC) transporter, which hydrolyzes ATP to transport substrates across membranes (6–9). Its topology suggests that ABCB10 exports one or more mitochondrial substrates into the cytoplasm. Abcb10 is essential for proper erythropoiesis and its loss is embryonic lethal due to increased apoptosis of erythroid precursor cells (6, 10). Recent work using ABCB10 reconstituted into liposomes indicates that biliverdin is one substrate that ABCB10 transports, and that hepatocytes lacking ABCB10 accumulate biliverdin inside mitochondria (11).

Here, we employed conditional knockout and CRISPR/Cas9 approaches to examine the effect of *Abcb10* deletion on T cell development, activation, proliferation and cytokine response in vitro and in vivo. We show that ABCB10 loss negatively impacts expression of TNFα and IL-2 in $CD4^+$ but not $CD8^+$ cells activated in vitro. In contrast, IFNγ is unaffected. Loss of ABCB10 progressively attenuates antiviral immune responses over time, with the largest effects observed during $CD4^+$ memory T cell formation and recall response. Malignant transformation frequently alters metabolism and metabolic requirements, suggesting that the effects of ABCB10 loss could differ in malignantly transformed cells. We used lentiviral CRISPR/Cas9 to ablate *Abcb10* in mouse EL4 cells, observing decreased proliferation in polyclonal knockout cells, and an inability to isolate knockout clones in standard media. In contrast, *Abcb10* knockout human Jurkat T cell clones could be derived, and these also showed severe deficiencies in TNFα and IL-2 but not IFNγ expression in response to activation. Metabolic profiling of these cells revealed a significant loss of mitochondrial oxidative capacity, coupled with a complete inability to switch to aerobic glycolysis upon stimulation. These results identify a selective requirement for ABCB10 in $CD4^+$ T cells to maintain stable memory T cell pools over time, and identify a strong ABCB10 requirement in malignantly transformed $CD4^+$ T cells. These findings have implications for halting overactive immune responses, and for treating T cell malignancies.

Materials and Methods

Mice

All animals were C57BL/6 background. Animal experiments were approved by the University of Utah Institutional Animal Care and Use Committee (IACUC approval 20–03002). The *Abcb10* conditional (floxed) allele has been described previously (11). Conditional mice were crossed to CD4-Cre (12) to delete *Abcb10* in the double-positive thymic compartment and their more mature progeny. Deletion was confirmed by TaqMan qRT-PCR using established methods (13).

Culture of primary T cells and cell lines

Primary T cells were cultured in RPMI 1640 medium supplemented with 10% FCS and 50 Units/mL penicillin, 50 μg/mL streptomycin, 2 mM L-glutamine, 1mM sodium pyruvate, 1X MEM non-essential amino acids, 55 mM 2-mercaptoethanol and 20 IU/mL recombinant IL-2. All components were from ThermoFisher with the exception of IL-2 which was supplied by R&D Systems. WT and *Abcb10* CRISPR/RNP $CD4^+$ T cells were cultured in RPMI1640 medium as described above with supplemental recombinant mouse IL-7 (Shenandoah Biotechnology) at 5 ng/mL. EL4 and Jurkat cells (ATCC) were cultured in RPMI 1640 with 15% FBS, 1X glutamax (Sigma) and pen/strep.

CRISPR/Cas9 mediated Abcb10 knockout in primary $CD4^+$ T cells

CRISPR guide RNAs were chosen targeting the 5' exons of the *Abcb10* gene using the IDT predesigned CRISPR guide RNA database (https://www.idtdna.com/site/order/designtool/index/CRISPR_PREDESIGN): *Abcb10*: GAGGTAGACACGAATGCCGTtgg; CCCAAGGTCTCGCACACCGGtgg; GGTCCACGCGCGTACGAGCGggg. Lower-case letters represent the PAM site. CRISPR/Cas9 negative control crRNA (IDT, 1072544) was used as a control for transfection. Nonspecific or *Abcb10*-specific CRISPR/Cas9 RNPs were generated from tracrRNA-ATTO550 (IDT), crRNA (IDT) and Cas9 protein (QB3 MacroLab, UC Berkeley) using commercial guidelines (IDT), and transfected into $CD4^+$ T cells purified from mouse spleens using a negative selection $CD4^+$ T cell isolation kit (Miltenyi Biotec). Transfection was accomplished by electroporation using the Neon transfection system 10 μL kit (ThermoFisher Scientific). Electroporation parameters were 2050V, 10 ms pulse width, 3 pulses. Transfection efficiency was measured by flow cytometry two days post-transfection to detect the tracrRNA-ATTO550 positive cells. Approximately 95% transfection efficiency was obtained. Viable, ATTO550 positive cells were sorted on the following day and adoptively transferred into recipient mice. Remaining cells were cultured for >5 days to confirm stable ablation of *Abcb10* mRNA by TaqMan RT-qPCR.

$LCMV^{Arm}$ Infection and Lm-GP61 re-challenge

Armstrong strain lymphocytic choriomeningitis virus ($LCMV^{Arm}$) infection and Lm-GP61 rechallenge were performed as described previously (14).

CRISPR/Cas9 mediated Abcb10 knockout in mouse EL4 T cells and human Jurkat cells

CRISPR lentiviral constructs were generated by the University of Utah Mutation Generation and Detection Core (http://cihd.cores.utah.edu/mgd/#1472062761315-b8a8c4eb-1a00). CRISPR expression lentiviral with GFP, BFP or mCherry were packaged in HEK293T cells using a three-plasmid packaging system. The supernatant containing retroviruses was passed through 0.45 μm filter and stored in aliquots at −80˚C. EL4 mouse T cells were transduced with CRISPR lentiviruses that targeted exon 1 (E1S2) CTCGTACGCGCGTGGACCTC or exon 3 (E3S9) TCGGATACCGCACTCC of the mouse *Abcb10* gene and 8 μg/mL of polybrene, and grown for two days in growth media. Transduced cells were sorted by flow cytometry for GFP-positive cells (*Abcb10*) or mCherry (Control) and single cells seeded into 96-well plates for development of clones that were mutated at the *Abcb10* locus. (No

EL4 GFP positive clones were able to be isolated). Human Jurkat E6.1 cells were transduced with CRISPR lentiviruses that targeted exon 1 (E1S1) GTCGCACGCAGCGCCATGCG, sorted for BFP (human *ABCB10*) or mCherry (Control) and single cells seeded and clones isolated.

RT-qPCR

mRNA was extracted using the RNeasy kit (Qiagen). 2 μg of total RNA was used to synthesize cDNA using the High Capacity cDNA reverse transcription kit (AB Biosystems). Power SYBR Green Master Mix (Life Technologies) was used on a Realplex2 real-time thermal cycler (Eppendorf). β-actin *ACTB* was used as a control housekeeping gene. The ΔΔCt method was used to compare the variation of transcripts among samples. Primers were validated by cloning and sequencing the PCR products.

RT-qPCR for human genes (*ABCB10*, *ACTB*, *IL-2*, *INFG* and *TNF*) and mouse genes (*IL-2, TNFa, INFg, Abcb10* and β-actin) was performed using PowerUp SYBR Green Master mix (Life Technologies) and primers are listed in Supplementary Table 1.

T cell activation and IL-2 ELISA

T cells were activated with PMA and ionomycin Cell Activation Cocktail (Biolegend) or using 10 μg/mL plate-bound CD3ε (Invitrogen) and 2 μg/mL soluble CD28 antibody (Invitrogen). Control and *ABCB10* mutant Jurkat cells were grown in growth medium ±25 μl/mL anti-CD3/CD28 for 24–72 hr according to the manufacturer's instructions. Media were harvested and secreted mouse IL-2 levels determined using an ELISA kit (Life Technologies) according to the manufacturer's instructions.

Immunoblotting

To isolate membranes, cell pellets were suspended in 0.25 M sucrose, 150 mM NaCl, 10 mM Tris-HCl pH 7.2, 0.5 mM EDTA 0°C and homogenized using a ball-bearing homogenizer. Homogenates were centrifuged at 400×*g* for 5 min, and supernatants centrifuged at 12,000×*g* for 30 min. Obtained membranes were lysed in 1% Triton X-100, 150 mM NaCl, 10 mM Tris-HCl pH 7.2, 0.5 mM EDTA with 2X Roche protease inhibitor tablets at 0°C for 30 min, and centrifuged at 15,000×*g* for 30 min at 4°C. Mitochondria were isolated from *Abcb10fl/fl* and *Abcb10fl/flCD4-Cre* primary T cells using a kit from ThermoFisher (89874). For primary T cell Abcb10 Western blots, T cells from three genotypically matched mice were pooled to permit for mitochondrial isolation and Abcb10 detection. Protein determinations were performed on membrane lysates using BCA assays (Pierce). Samples were resolved by electrophoresis through 4–20% Tris-glycine SDS-PAGE gels, transferred to nitrocellulose and probed using primary antibodies against Abcb10 (1:500 ThermoFisher), VDAC1 (1:1000, Abcam) and Horseradish peroxidase conjugated goat anti-rabbit or mouse IgG was used as a secondary (1:5000, Jackson ImmunoResearch). Western blots were developed using Western Lightening Reagent (PerkinElmer Life Sciences), and blots were quantified using Fiji Image J software. Statistical analyses were performed using Student's t test unless otherwise stated. Significance of $p \leq 0.05$ is shown as an asterisk.

Seahorse Analysis

Control (mCherry) and *ABCB10* disrupted Jurkat cells were activated as described (12 biological replicates) and 2×10^5 cells per well seeded, centrifuged at 1500×*g* for 10 min and incubated for 20–60 min 37°C in a non-CO_2 incubator. Following initial incubation, XF Running Media (XF assay media with 5% FCS and 10 mM D-glucose) were dispensed into each well. OCR and ECAR were measured by an XF96 Seahorse Extracellular Flux Analyzer following the manufacturer's instructions. Cells were treated with oligomycin (1.0 μM), FCCP (1.5 μM), rotenone (100 nM) and antimycin A (1.0 μM) as per manufacturer's instructions. Each condition was performed in 2–3 technical replicates. Subsequent protein determinations were performed to normalize the results to protein levels (μg/mL). Because the DAPI staining procedure and washes to count cells within the Seahorse plate can make Jurkat cells detach and thus underestimate real cell count by imaging, the safest procedure to get the most accurate cell counts is to aspirate the media after the assay and add lysis buffer directly to the well, to measure total protein content per well.

Statistical Analysis

For animal studies a minimum of 3 mice per group were used. The number of experimental replicates is stated in the figure legends. All in vitro experiments and cell culture experiments were performed with a minimum of three biologic replicates. Statistical analyses were performed using Student's t test unless otherwise stated. Significance of $p \leq 0.05$ is shown as an asterisk.

Results

Conditional Abcb10 deletion in T cells is compatible with development and short-term in vitro responses

Previous work showed that an *Abcb10* conditional (floxed) mouse allele could be efficiently deleted using Albumin-Cre, resulting in the accumulation of biliverdin inside mitochondria and the elevation of mitochondrial OXPHOS in livers from diet-induced obese mice (11). To delete *Abcb10* in T cells, we crossed *Abcb10* floxed mice to CD4-Cre (12), which express Cre in developing T cells starting at the CD4/CD8 double-positive stage. Using TaqMan qRT-PCR with total splenic T cells and either of two different intron-spanning primer-pairs specific to *Abcb10*, we observed significant decreases in *Abcb10* relative to β-actin mRNA in total *Abcb10*$^{fl/fl}$;CD4-Cre splenic T cells (Fig. 1A). Using preparations of mitochondria purified from primary T cells, we also observed a corresponding loss of Abcb10 protein (Fig. 1B). Inspection of the thymocytes from *Abcb10*$^{fl/fl}$;CD4-Cre mice revealed no differences in either percentages or absolute numbers of double-negative, double-positive or single-positive cells relative to *Abcb10*$^{fl/fl}$ controls lacking CD4-Cre (Supp. Fig. 1A–C). In the periphery, total splenic and inguinal lymph node $CD4^+$ and $CD8^+$ cells were also present in normal numbers in specific pathogen-free mice (Supp. Fig. 1D–E). Isolating these cells and stimulating them in vitro using PMA and ionomycin resulted in equivalent expression of the cytokine IFNγ, but significantly reduced levels of TNFα and IL-2 specifically in $CD4^+$ cells. Interestingly, no diminution was observed in $CD8^+$ cells, or for IFNγ in $CD4^+$ cells (Fig. 1C). Similar results were obtained by RT-qPCR (Supp. Fig. 1F). In specific pathogen-free mice, the purified cells were mostly (80%) naïve

phenotype ($CD62L^{hi}CD44^{lo}$) regardless of genotype (data not shown). We also stimulated total splenic T cells in vitro for two days using plate-bound CD3ε and soluble CD28 antibodies, and measured proliferation using cell trace violet (CTV). Both $CD8^+$ and $CD4^+$ *Abcb10*$^{fl/fl}$;CD4-Cre T cell populations proliferated equivalently to controls (Supp. Fig. 1G). These results indicate that ABCB10 is dispensable for thymocyte development past the double-positive stage and for peripheral T cell survival in vivo, as well as for survival and proliferation following in vitro stimulation. However, ABCB10 is required for robust expression of a subset of cytokines in $CD4^+$ T cells in vitro.

To study T cell antigen response in a physiological situation, we infected *Abcb10*$^{fl/fl}$;CD4-Cre mice with $LCMV^{Arm}$, and studied their T cell responses to virus and viral titers. Normal infected mice activate $CD4^+$ and $CD8^+$ T cells, clear the pathogen within 10 days, and generate stable memory T cell populations (15). At peak (D8) LCMV response, we noted decreased percentages of $CD4^+$ populations relative to $CD8^+$ in *Abcb10*$^{fl/fl}$;CD4-Cre mice (Fig. 1D). Similar findings were made gating specifically on activated $CD44^+$ cells (Fig. 1D). Quantifying absolute numbers of cells indicated both a trend toward decreased total $CD4^+$ cell numbers, and significant increases in $CD8^+$ cell numbers induced by ABCB10 deletion (p=0.0022, Fig. 1E). To study antigen-specific antiviral responses, we used MHC class I and II tetramers corresponding to LCMV immunodominant epitopes at D8. Using either class II and class I tetramers, we observed few differences in the percentage of virus-specific responding T cells (Fig. 1F). Quantification of total tetramer-positive cells also showed few differences, however, there was a trend toward increased numbers of $CD8^+$ cells compared to controls (Fig. 1G). We also determined viral titers during the infection time course, identifying no changes due to ABCB10 loss (Fig. 1H). In addition, the expression of specific activation markers (CD44, CD62L, ICOS, PD-1, Ly6C) was unchanged (data not shown).

Impairment of in vivo memory responses in the absence of Abcb10

The formation of CD4 memory requires dynamic changes in metabolism, including a shift from proliferative, glycolytic metabolism to a metabolic state dominated by fatty acid oxidation (1, 16). We allowed mice to clear LCMV and monitored their resting splenic memory T cells 45 days post-infection. As expected, there were no differences in total $CD4^+$ and $CD8^+$ T cells, most of which are not antigen-specific (Fig. 2A). Antigen-specific (tetramer-positive) $CD4^+$ and $CD8^+$ memory T cells were slightly fewer in number in the absence of ABCB10, though this was not statistically significant (Fig. 2B). We then rechallenged the mice with recombinant *Listeria monocytogenes* expressing a fragment of the LCMV glycoprotein ($GP_{61–80}$) that elicits a strong $CD4^+$ response (Lmgp61). Following rechallenge (day 45+7), we observed no differences in total $CD4^+$ and $CD8^+$ T cells but a robust decline in antigen-specific $CD4^+$ numbers, both as a percentage of total T cells and in terms of absolute numbers (Fig. 2C, D). Cumulatively, these results indicate a progressive loss of $CD4^+$ T cell potential over time.

Acute and conditional Abcb10 knockout in T cells reduces production of specific cytokines and decreases memory CD4 responses

Recent advances in CRISPR/Cas9 technology, T cell transfection, and fluorophore-conjugated trcrRNAs allow for rapid gene knockout generation in mouse and human primary T cells (17). We employed a system with Cas9 enzyme, CRISPR RNA ("crRNA", which contains the DNA-binding "protospacer" sequence), and fluorescently-conjugated trans-activating CRISPR RNA ("trcrRNA", which binds Cas9). In this system, the three reagents are transfected as a ribonucleoprotein (RNP) complex into T cells. No prior T cell activation is required and this transfection method shows 90–95% efficiency in primary mouse T cells. After 24 hr of treatment with recombinant IL-7, transfected cells were sorted using the fluorescent trcrRNA conjugate. Following sorting, cells were tested for knockout efficiency in culture or adoptively transferred into recipient mice. We successfully used these methods to knockout *Cd90* (*Thy1*) in primary T cells (Supp. Fig. 2A/B). We then adapted this strategy to target *Abcb10* and examine cells subjected to repeated stimulation in vitro. Cells transfected with *Abcb10*-specific but not control gRNAs showed significant decreases in *Abcb10* mRNA expression, as measured by TaqMan RT-qPCR using two different primer-pairs (Fig. 3A). Stimulation of primary $CD4^+$ T cells in culture with plate-bound CD3ε and soluble CD28 antibodies, followed by resting in the presence of IL-2 and restimulation, results in stronger and broader cytokine responses (14, 18, 19). We stimulated primary T $CD4^+$ cells ($CD8a^{neg}CD11b^{neg}CD11c^{neg}CD19^{neg}CD45R^{neg}DX5^{neg}CD105^{neg}MHCII^{neg}Ter\text{-}119^{neg}TCR\gamma/\delta^{neg}$) that had been transfected with *Abcb10*-specific or control gRNAs for two days, rested them for 8 additional days before restimulating the cells for 12 hr. Restimulated *Abcb10*-deficient T cells showed significantly decreased IL-2 but not IFNγ expression (Fig. 3B). Stronger effects were found with Cre-mediated conditional knockout using the same stimulate-rest-restimulate conditions (Fig. 3C).

To test effects of *Abcb10* deficiency in vivo, we performed similar CRISPR-mediated gene knockouts using SMARTA TCR transgenic T cells, adoptively transferred them into recipient mice, and measured their responses to acute infection with lymphocytic choriomeningitis virus (LCMV), an arenavirus and widely used model pathogen. SMARTA cells recognize a CD4 immunodominant epitope of LCMV, undergoing multiple rounds of division while gaining Th1 effector functionality normally characterized by IFNγ and IL-2 expression (20). We transfected $Ly5.1^+$ ($CD45.1^+$) $CD4^+$ T cells with *Abcb10*-specific crRNAs, and and $Ly5.1^+/Ly5.2^+$ control T cells with crRNAs, combined them 1:1, and transferred them into $Ly5.2^+$ recipient animals. Recipients were then infected with the Armstrong strain of LCMV. Prior to transfer at D0, equivalent numbers of nonspecific and *Abcb10* RNP cells were present as measured by flow cytometry (Fig. 3D). After transfer and at peak response to LCMV (D8), the ratio of cells transfected with *Abcb10* to nonspecific RNPs (lower right vs. upper right quadrants) remained close to 1:1. Following antigen re-exposure using infection with Lmgp61 expressing the same LCMV immunodominant epitope (D42+7), the *Abcb10*/control RNP ratio dropped significantly (Fig. 3D, E). This result indicates that $CD4^+$ T cell memory recall responses are reduced in the absence of ABCB10.

We also crossed *Abcb10*$^{fl/fl}$ and CD4-Cre mice to the SMARTA transgene and to the Ly5.1 congenic marker, allowing us to discriminate experimental and control SMARTA cells from each other and from Ly5.1 recipient T cells. Ly5.2 *Abcb10*$^{fl/fl}$;CD4-Cre cells were combined 1:1 with control Ly5.1/5.2 *Abcb10*$^{fl/fl}$ cells, and verified by flow cytometry prior to T cell transfer (Fig. 3F,G). Following infection with LCMV, the ratio of Splenic SMARTA cells at peak response showed a slight skewing toward control at the expense of Abcb10 deficient T cells (D8). Strikingly, both resting memory cells in mice 42 days after infection, and cells mounting a recall response in mice rechallenged with Lmgp61 showed ~10-fold diminution in experimental relative to control cells (D42 and D42+7). Unlike the polyclonal response (Fig. 2), the SMARTA transgenic recognizes a single immunodominant LCMV CD4 epitope. The increased severity of the phenotype relative to polyclonal *Abcb10* conditional mice (Fig. 2) likely explains the effects on resting memory cells as well as cells undergoing recall responses. These results are consistent with the progressive attrition in the ability of T cells lacking Abcb10 to respond to LCMV, form memory and mount recall responses.

Loss of Abcb10 in human Jurkat cells reduces activation and blocks activation-induced metabolic switching

To determine if loss of ABCB10 affected malignant T cell growth or activation, we transduced mouse EL4 T cells or human Jurkat cells with *Abcb10/ABCB10*-specific or control CRISPR/Cas9 lentiviruses expressing fluorescent markers. Cells were sorted by flow cytometry and pools of control lentivirus-infected (mCherry^{+}) or *Abcb10* CRISPR lentivirus-infected (GFP^{+}) cells were grown in normal tissue culture medium for 48 hr to assess proliferative capacity. Pooled *Abcb10* CRISPR EL4 cells showed a marked reduction in proliferation (Fig. 4A). Pools of cells were single cell sorted into 96-well plates to isolate control and *Abcb10/ABCB10* mutant clones. We successfully isolated Jurkat clones (control and *ABCB10* mutants) as well as EL4 control clones, however, we were unable to isolate EL4 *Abcb10* mutant clones (Supp. Table 2) limiting our ability to further assess loss of ABCB10 in these cells. We therefore focused on two independent Jurkat clones (A1 and A3) that showed dramatic reductions in ABCB10 protein (Fig. 4B). There was no difference in cell proliferation in *ABCB10* mutants compared to control cells (Fig. 4C). When Jurkat cells were activated by anti-CD3/CD28, *ABCB10* mutants showed reduced IL-2 secretion compared to control Jurkat cells (Fig. 4D). The *ABCB10* mutant line A3 showed the most dramatic reduction in IL-2 secretion upon activation. This reduction in IL-2 secretion was a result of diminished activation and not a reduction in secretion, as shown by the decrease in *IL-2* transcripts. Loss of ABCB10 also resulted in a significant reduction in *TNFA* transcripts and a trend toward reduced *INFG* transcripts (Fig. 4E) supporting a role for human ABCB10 in T cell activation in malignant cells.

As malignant cells rely heavily on OXPHOS, which requires efficient Fe-S cluster (ISC) and heme synthesis, we hypothesized that loss of ABCB10 would affect mitochondrial metabolism. We measured mitochondrial OXPHOS using resting and activated (anti-CD3/CD28) WT and *ABCB10* mutant Jurkat cells (A3) monitoring oxygen consumption using the Seahorse Extracellular Analyzer. WT cells (C1) showed a marked reduction in oxygen consumption rate (OCR) upon activation (Fig. 5A circles), as well as in extracellular

acidification rate (ECAR, Fig. 5B, circles). When primary T cells are activated, OXPHOS is known to go down and glycolysis increase (21). This concurrent decrease in ECAR in Jurkat cells is expected when CO_2 production from the mitochondrial TCA cycle is the major contributor to ECAR. Despite inducing a mild reduction in respiration before activation, loss of ABCB10 (A3) resulted in an inability to reduce oxygen consumption in response to activation (Fig. 5A triangles). Accordingly, basal respiration was markedly reduced in activated WT Jurkat cells (Fig. 5C, C1), while cells lacking Abcb10 showed little diminution upon activation (Fig. 5C, A3**).** ATP-linked respiration, proton leak, maximal respiratory capacity and spare respiratory reserve showed similar trends with significant reductions upon activation in WT cells and minimal shifts in these parameters in *ABCB10* mutant cells. These results support the interpretation that ABCB10 promotes the ability to shift oxidative metabolism during malignant T cell activation.

Discussion

Here we show that loss of the mitochondrial ATP binding cassette transporter ABCB10 in mouse T cells has no effect on T cell development, or on peripheral T cell survival/stability in resting mice, but results in $CD4^+$-selective defects in peripheral T cell functionality. $CD4^+$ T cells also become depleted at later timepoints associated with immune memory. Metabolic profiling of human Jurkat T cell clones deficient in ABCB10 reveals defects in metabolic remodeling induced by activation, supporting an interpretation that these defects are metabolic in nature. The metabolic states of effector and memory T cells are known to differ from one another, and from T cell development (1, 16). For example, during an immune response memory precursor cells must shift their metabolism from a predominantly glycolytic profile used to sustain proliferative and effector functions, to a profile highly reliant on fatty acid oxidation that more efficiently generates ATP per mol of nutrient. Our results suggest that substrates transported by ABCB10 may be required for these shifts.

Primary ABCB10 KO T cell stimulation in vitro revealed no changes in proliferation or the production of cytokines in $CD8^+$ cells, but did result in cytokine production defects in ABCB10 KO $CD4^+$ cells. Interestingly, the defects in cytokine production were also selective in nature. TNFα and IL-2 were significantly decreased, whereas IFNγ was unaltered. These results were recapitulated and magnified in human Jurkat cells with CRISPR-mediated *ABCB10* knockout.

We found few changes in ABCB10 deficient polyclonal T cells at peak response to LCMV, but using a heterologous rechallenge system we observed large differences. Using a SMARTA transgenic system, we also observed significant decreases in $CD4^+$ T cell numbers at memory and memory recall response. $CD4^+$ T cells are known to undergo a series of metabolic alterations as they transition from naïve to effector or memory cells (22). Overall these findings indicate a decline in the fitness of ABCB10-deficient T cells over time in vivo, and suggest that this observation may be linked to failure of T cells to undergo metabolic adaptation.

Recent advances in CRISPR/Cas9 technologies enable efficient ablation of specific target genes in primary lymphocytes using transfected ribonucleoproteins (17, 23, 24). We

employed this system to acutely delete Abcb10 in primary $CD4^+$ T cells. We observed significant decreases in cytokine expression in response to secondary stimulation as observed in conditional mice. CRISPR methods also allow for the rapid deployment of Abcb10 knockouts into genetically modified T cells, such as SMARTA transgenic T cells. Using these cells allows for easy monitoring of their responses to LCMV. Using T cell adoptive transfer and congenic markers, we showed that Abcb10 loss selectively depletes antigen-specific T cell memory recall responses. These findings support those made using a conditional *Abcb10* allele, and indicate that they are not due to development in an Abcb10-deficient environment.

We employed CRISPR/Cas9 methods to delete *Abcb10/ABCB10* in malignant mouse EL4 and human Jurkat T cells. *Abcb10*-targeted EL4 cells showed a marked reduction in proliferation, which limited our ability to establish deletion clones for further analysis. However, we were able to establish *ABCB10* null Jurkat clones that proliferated normally. We observed that upon in vitro stimulation, the loss of Abcb10 limited transcriptional induction of both *IL2* and *TNFa* mRNA even more so than in nonmalignant T cells. Mitochondrial functional analyses revealed significant limitations for the metabolic remodeling known to occur upon T cell activation in the absence of ABCB10. Jurkat cells have disrupted PI3K pathway signaling due to the loss of PTEN expression, which may result in a persistent activated state (25). The potent effects of PI3K signaling on metabolism may provide an explanation for the observation that Jurkat cells activated for extended amounts of time (72hr) with anti-CD3/CD28 show an inability to increase glycolysis due to exhaustion. It is also possible that Jurkat cells do not rely on an increase in glycolysis for activation and cytokine production. Previous studies support that the blockage of OXPHOS can induce the accumulation of TCA intermediates (reviewed in (26)). These intermediates can then translocate to the cytosol, to cause changes in histone acetylation, as well as direct actions on transcriptional regulators, to elevate cytokine expression. Thus, our findings support that ABCB10 activity might be specifically needed to induce the accumulation of TCA cycle intermediates to increase the expression of cytokines. Importantly, WT Jurkat reduced OXPHOS upon stimulation, whereas the loss of ABCB10 prevented this reduction in OXPHOS suggesting that ABCB10 loss alters mitochondrial metabolism. ABCB10 exports biliverdin to the cytosol, which results in increased bilirubin synthesis and decreased OXPHOS in hepatocytes (11). Based upon these observations and our results in $CD4^+$ T cells, we speculate that ABCB10 decreases OXPHOS by increasing bilirubin levels. Thus, a lack of bilirubin synthesis stimulation after T cell activation due to loss of ABCB10 may explain the observation that defects manifest subsequent but not prior to T cell activation.

In summary, our results show that ABCB10 is dispensable for T cell development and activation, but required for expression of specific cytokines with the $CD4^+$ T cell compartment. Further, loss of ABCB10 affects $CD4^+$ T cell memory formation and recall responses and it is critical to metabolic reprogramming. The phenotypes tend to be more dramatic in some malignant T cells, suggesting that ABCB10 may be a targetable node to modulate T cell metabolism in malignant cells while sparing at least some baseline T cell functions. Future studies will focus on determining the defects in memory formation in $CD4^+$ T cells in the absence of ABCB10.

Supplementary Material

Refer to Web version on PubMed Central for supplementary material.

Acknowledgements

We thank S. Hale for critical reading of the manuscript.

This work was supported by a departmental seed grant to DMW and DT, NIH grant R01AI100873 to DT, NIH grant U54DK110858 to DMW and NIH grant R01AA026914 to ML.

References

1. Almeida L, Lochner M, Berod L, and Sparwasser T. 2016. Metabolic pathways in T cell activation and lineage differentiation. Semin Immunol 28: 514–524. [PubMed: 27825556]
2. Ma EH, Bantug G, Griss T, Condotta S, Johnson RM, Samborska B, Mainolfi N, Suri V, Guak H, Balmer ML, Verway MJ, Raissi TC, Tsui H, Boukhaled G, Henriques da Costa S, Frezza C, Krawczyk CM, Friedman A, Manfredi M, Richer MJ, Hess C, and Jones RG. 2017. Serine Is an Essential Metabolite for Effector T Cell Expansion. Cell Metab 25: 345–357. [PubMed: 28111214]
3. O'Sullivan D, van der Windt GJ, Huang SC, Curtis JD, Chang CH, Buck MD, Qiu J, Smith AM, Lam WY, DiPlato LM, Hsu FF, Birnbaum MJ, Pearce EJ, and Pearce EL. 2014. Memory CD8(+) T cells use cell-intrinsic lipolysis to support the metabolic programming necessary for development. Immunity 41: 75–88. [PubMed: 25001241]
4. O'Sullivan D, van der Windt GJW, Huang SC, Curtis JD, Chang CH, Buck MD, Qiu J, Smith AM, Lam WY, DiPlato LM, Hsu FF, Birnbaum MJ, Pearce EJ, and Pearce EL. 2018. Memory CD8(+) T Cells Use Cell-Intrinsic Lipolysis to Support the Metabolic Programming Necessary for Development. Immunity 49: 375–376. [PubMed: 30134202]
5. van der Windt GJ, and Pearce EL. 2012. Metabolic switching and fuel choice during T-cell differentiation and memory development. Immunol Rev 249: 27–42. [PubMed: 22889213]
6. Hyde BB, Liesa M, Elorza AA, Qiu W, Haigh SE, Richey L, Mikkola HK, Schlaeger TM, and Shirihai OS. 2012. The mitochondrial transporter ABC-me (ABCB10), a downstream target of GATA-1, is essential for erythropoiesis in vivo. Cell Death Differ 19: 1117–1126. [PubMed: 22240895]
7. Qiu W, Liesa M, Carpenter EP, and Shirihai OS. 2015. ATP Binding and Hydrolysis Properties of ABCB10 and Their Regulation by Glutathione. PLoS One 10: e0129772. [PubMed: 26053025]
8. Seguin A, Takahashi-Makise N, Yien YY, Huston NC, Whitman JC, Musso G, Wallace JA, Bradley T, Bergonia HA, Kafina MD, Matsumoto M, Igarashi K, Phillips JD, Paw BH, Kaplan J, and Ward DM. 2017. Reductions in the mitochondrial ABC transporter Abcb10 affect the transcriptional profile of heme biosynthesis genes. J Biol Chem 292: 16284–16299. [PubMed: 28808058]
9. Shintre CA, Pike AC, Li Q, Kim JI, Barr AJ, Goubin S, Shrestha L, Yang J, Berridge G, Ross J, Stansfeld PJ, Sansom MS, Edwards AM, Bountra C, Marsden BD, von Delft F, Bullock AN, Gileadi O, Burgess-Brown NA, and Carpenter EP. 2013. Structures of ABCB10, a human ATP-binding cassette transporter in apo- and nucleotide-bound states. Proc Natl Acad Sci U S A 110: 9710–9715. [PubMed: 23716676]
10. Yamamoto M, Arimura H, Fukushige T, Minami K, Nishizawa Y, Tanimoto A, Kanekura T, Nakagawa M, Akiyama S, and Furukawa T. 2014. Abcb10 role in heme biosynthesis in vivo: Abcb10 knockout in mice causes anemia with protoporphyrin IX and iron accumulation. Mol Cell Biol 34: 1077–1084. [PubMed: 24421385]
11. Shum M, Shintre CA, Althoff T, Gutierrez V, Segawa M, Saxberg AD, Martinez M, Adamson R, Young MR, Faust B, Gharakhanian R, Su S, Chella Krishnan K, Mahdaviani K, Veliova M, Wolf DM, Ngo J, Nocito L, Stiles L, Abramson J, Lusis AJ, Hevener AL, Zoghbi ME, Carpenter EP, and Liesa M. 2021. ABCB10 exports mitochondrial biliverdin, driving metabolic maladaptation in obesity. Sci Transl Med 13.
12. Lee PP, Fitzpatrick DR, Beard C, Jessup HK, Lehar S, Makar KW, Perez-Melgosa M, Sweetser MT, Schlissel MS, Nguyen S, Cherry SR, Tsai JH, Tucker SM, Weaver WM, Kelso A, Jaenisch

R, and Wilson CB. 2001. A critical role for Dnmt1 and DNA methylation in T cell development, function, and survival. Immunity 15: 763–774. [PubMed: 11728338]

13. Liesa M, Luptak I, Qin F, Hyde BB, Sahin E, Siwik DA, Zhu Z, Pimentel DR, Xu XJ, Ruderman NB, Huffman KD, Doctrow SR, Richey L, Colucci WS, and Shirihai OS. 2011. Mitochondrial transporter ATP binding cassette mitochondrial erythroid is a novel gene required for cardiac recovery after ischemia/reperfusion. Circulation 124: 806–813. [PubMed: 21788586]
14. Shakya A, Goren A, Shalek A, German CN, Snook J, Kuchroo VK, Yosef N, Chan RC, Regev A, Williams MA, and Tantin D. 2015. Oct1 and OCA-B are selectively required for CD4 memory T cell function. J Exp Med 212: 2115–2131. [PubMed: 26481684]
15. Jamieson BD, and Ahmed R. 1989. T cell memory. Long-term persistence of virus-specific cytotoxic T cells. J Exp Med 169: 1993–2005. [PubMed: 2471771]
16. Bailis W, Shyer JA, Zhao J, Canaveras JCG, Al Khazal FJ, Qu R, Steach HR, Bielecki P, Khan O, Jackson R, Kluger Y, Maher LJ 3rd, Rabinowitz J, Craft J, and Flavell RA. 2019. Distinct modes of mitochondrial metabolism uncouple T cell differentiation and function. Nature 571: 403–407. [PubMed: 31217581]
17. Seki A, and Rutz S. 2018. Optimized RNP transfection for highly efficient CRISPR/Cas9-mediated gene knockout in primary T cells. J Exp Med 215: 985–997. [PubMed: 29436394]
18. Murayama A, Sakura K, Nakama M, Yasuzawa-Tanaka K, Fujita E, Tateishi Y, Wang Y, Ushijima T, Baba T, Shibuya K, Shibuya A, Kawabe Y, and Yanagisawa J. 2006. A specific CpG site demethylation in the human interleukin 2 gene promoter is an epigenetic memory. EMBO J 25: 1081–1092. [PubMed: 16498406]
19. Shakya A, Kang J, Chumley J, Williams MA, and Tantin D. 2011. Oct1 is a switchable, bipotential stabilizer of repressed and inducible transcriptional states. J Biol Chem 286: 450–459. [PubMed: 21051540]
20. Oxenius A, Bachmann MF, Zinkernagel RM, and Hengartner H. 1998. Virus-specific MHC-class II-restricted TCR-transgenic mice: effects on humoral and cellular immune responses after viral infection. Eur J Immunol 28: 390–400. [PubMed: 9485218]
21. Guzik TJ, and Cosentino F. 2018. Epigenetics and Immunometabolism in Diabetes and Aging. Antioxid Redox Signal 29: 257–274. [PubMed: 28891325]
22. Araki K, Turner AP, Shaffer VO, Gangappa S, Keller SA, Bachmann MF, Larsen CP, and Ahmed R. 2009. mTOR regulates memory CD8 T-cell differentiation. Nature 460: 108–112. [PubMed: 19543266]
23. Roth TL, Puig-Saus C, Yu R, Shifrut E, Carnevale J, Li PJ, Hiatt J, Saco J, Krystofinski P, Li H, Tobin V, Nguyen DN, Lee MR, Putnam AL, Ferris AL, Chen JW, Schickel JN, Pellerin L, Carmody D, Alkorta-Aranburu G, Del Gaudio D, Matsumoto H, Morell M, Mao Y, Cho M, Quadros RM, Gurumurthy CB, Smith B, Haugwitz M, Hughes SH, Weissman JS, Schumann K, Esensten JH, May AP, Ashworth A, Kupfer GM, Greeley SAW, Bacchetta R, Meffre E, Roncarolo MG, Romberg N, Herold KC, Ribas A, Leonetti MD, and Marson A. 2018. Reprogramming human T cell function and specificity with non-viral genome targeting. Nature 559: 405–409. [PubMed: 29995861]
24. Chu VT, Graf R, Wirtz T, Weber T, Favret J, Li X, Petsch K, Tran NT, Sieweke MH, Berek C, Kuhn R, and Rajewsky K. 2016. Efficient CRISPR-mediated mutagenesis in primary immune cells using CrispRGold and a C57BL/6 Cas9 transgenic mouse line. Proc Natl Acad Sci U S A 113: 12514–12519. [PubMed: 27729526]
25. Shan X, Czar MJ, Bunnell SC, Liu P, Liu Y, Schwartzberg PL, and Wange RL. 2000. Deficiency of PTEN in Jurkat T cells causes constitutive localization of Itk to the plasma membrane and hyperresponsiveness to CD3 stimulation. Mol Cell Biol 20: 6945–6957. [PubMed: 10958690]
26. Ryan DG, Murphy MP, Frezza C, Prag HA, Chouchani ET, O'Neill LA, and Mills EL. 2019. Coupling Krebs cycle metabolites to signalling in immunity and cancer. Nat Metab 1: 16–33. [PubMed: 31032474]
27. Dier U, Shin DH, Hemachandra LP, Uusitalo LM, and Hempel N. 2014. Bioenergetic analysis of ovarian cancer cell lines: profiling of histological subtypes and identification of a mitochondria-defective cell line. PLoS One 9: e98479. [PubMed: 24858344]

Key Points:

- *ABCB10* null CD4 T but not CD8 T cells produce less IL-2 and TNFα upon activation.
- $CD4^+$-specific loss of *Abcb10* results in poor memory formation and recall responses.
- *ABCB10* null Jurkat T cells do not switch to glycolysis upon activation.

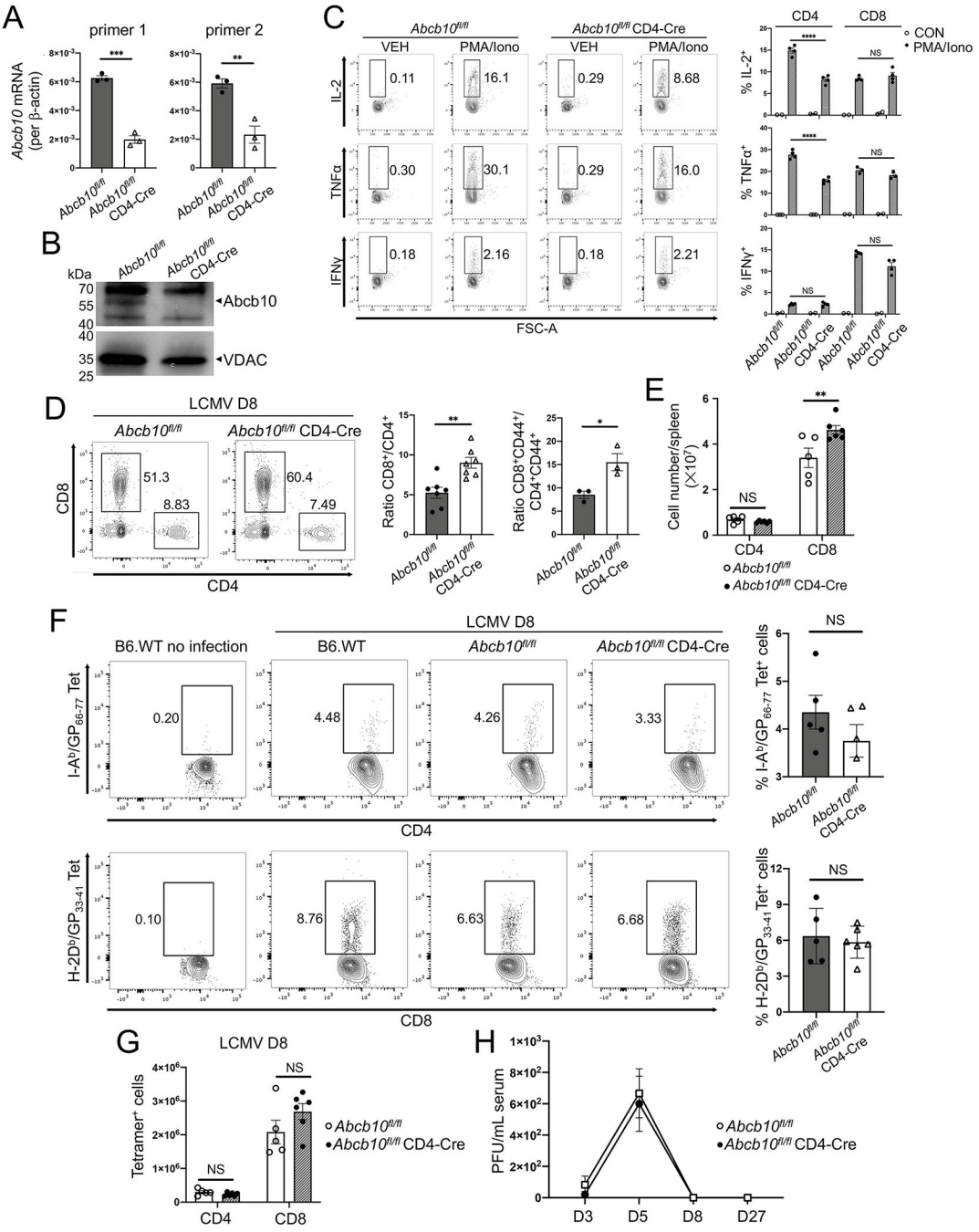

FIGURE 1.

Abcb10 T cell conditional knockout results in normal resting T cell pools but defective expression of select cytokines following stimulation of $CD4^+$ cells in vitro. **(A)** Total RNA from purified total $CD4^+$ T cells from *Abcb10*$^{fl/fl}$ and *Abcb10*$^{fl/fl}$ CD4-Cre mice was subjected to *Abcb10* RT-qPCR using TaqMan primers. Expression levels are shown relative to β-actin internal standard. Error bars depict ±SEM. (n=3 biologic replicates). This experiment was repeated once with similar results. **(B)** Mitochondrial were isolated from *Abcb10*$^{fl/fl}$ and *Abcb10*$^{fl/fl}$ CD4-Cre mouse T cells, a pool of n=3 from each genotype, and

Abcb10 and VDAC levels determined by Western blot. A representative blot is shown. The arrowhead denotes the band that is lost in *Abcb10*$^{fl/fl}$ CD4-Cre mouse T cells. **(C)** Total T cells were purified with pan T cell purification kit, cells were stimulated with a PMA/Ionomycin cell activation cocktail for 8 hr, and tested by flow cytometry for intracellular IL-2, TNFα and IFNγ, gating on CD4$^+$ or CD8$^+$ (data not shown). The percentage of IL-2$^+$, TNFα$^+$ and IFNγ$^+$ of CD4$^+$ and CD8$^+$ T cells are summarized in bar graphs at right. Each symbol represents a biological replicate (n=4). Error bars depict ±SEM. **(D)** *Abcb10*$^{fl/fl}$ and *Abcb10*$^{fl/fl}$ CD4-Cre mice were infected i.p. with 2×10^5 pfu LCMV^{Arm}. At peak response (D8), splenic CD4$^+$ and CD8$^+$ were quantified by flow cytometry. Quantification of total CD8$^+$/CD4$^+$ and activated CD8$^+$CD44$^+$/CD4$^+$/CD44$^+$ are shown as bar graphs. Each symbol represents a mouse (n=3–7 biologic replicates). **(E)** Total CD4$^+$ and CD8$^+$ numbers from (D) were quantified. Each symbol represents a mouse (n=5–6 biologic replicates). Error bars depict ±SEM. **(F)** Splenocytes from mice in (D) were stained with MHCII-peptide ($GP_{66–77}$ DIYKGVYQFKSV) or MHCI-peptide (GP var C41M 33–41 KAVYNFATM) tetramers to detect antigen-specific CD4$^+$ and CD8$^+$ T cells at D8 peak response. Total tetramer-positive CD4$^+$ and CD8$^+$ T cells per spleen are quantified at right. Each symbol represents one mouse and error bars depict ±SEM. (n=4–6 biologic replicates). **(G)** Total tetramer-positive CD4$^+$ and CD8$^+$ numbers from (F) were quantified. Error bars depict ±SEM. Each symbol represents a mouse (n=5–6 biologic replicates). **(H)** Serum viral titers were measured at D3, D5, D8 and D27 post-infection by plaque assay. Titers from 5 (*Abcb10*$^{fl/fl}$) and 6 (*Abcb10*$^{fl/fl}$ CD4-Cre) mice were averaged and error bars depict ±SEM.

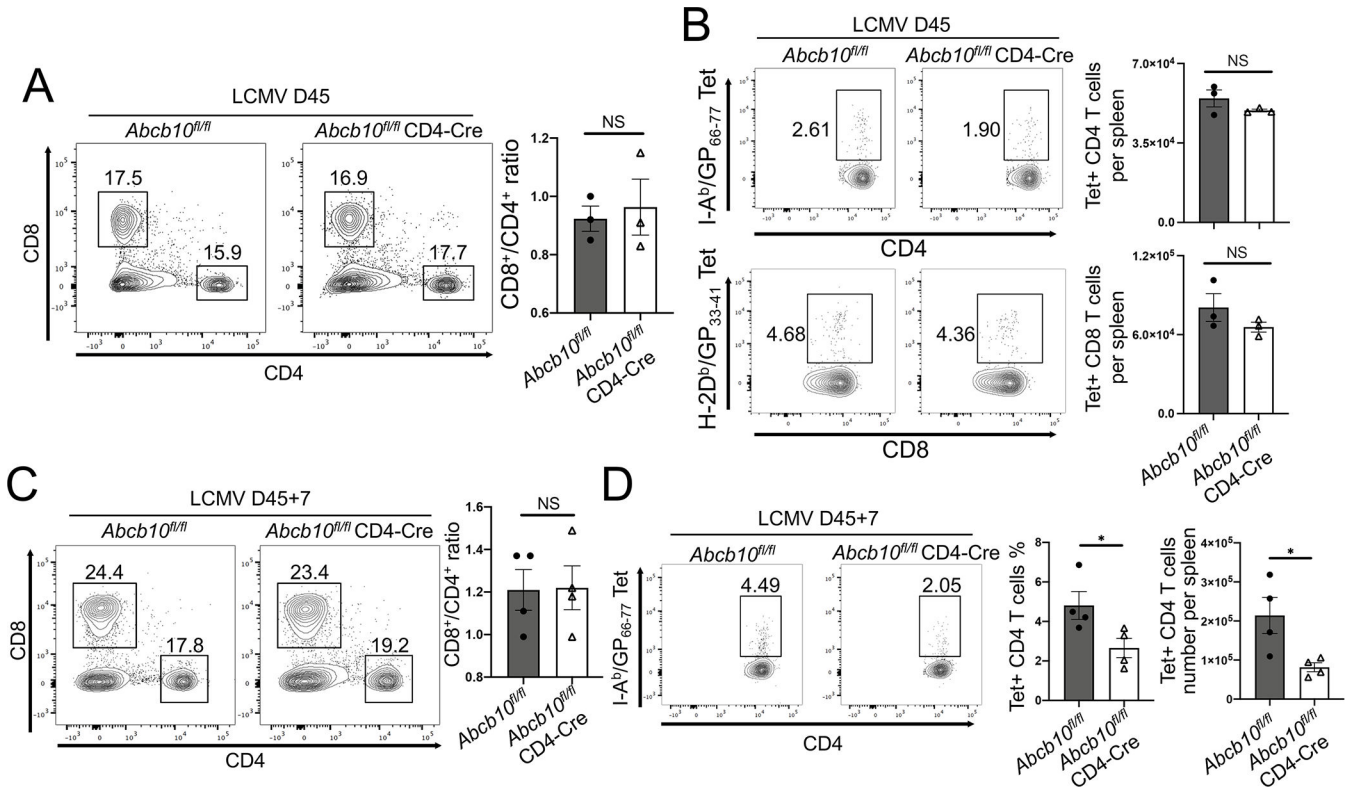

FIGURE 2.

Abcb10 T cell conditional knockout results in reduced T cell recall response. **(A-D)** Three or four mice in each group indicated were challenged with LCMV (Armstrong) and rested for 45 days, then challenge with Lm-GP 61 for 7 days. **(A, C)** CD4 and CD8 cell populations of splenocytes at day 45 and day 45+7 were showed by flow. $CD8^+/CD4^+$ T cells ratio was summarized as bar graph on the right. **(B, D)** Splenocytes were used for MHCII or MHCI tetramer staining for flow analysis. On the right side, MHCII tetramer + $CD4^+$T cells numbers and percentage, MHCI tetramer + $CD8^+$T cells numbers are summarized as bar graphs. Each symbol represents one mouse. Error bars depict ±SEM. (n=3–4 biologic replicates).

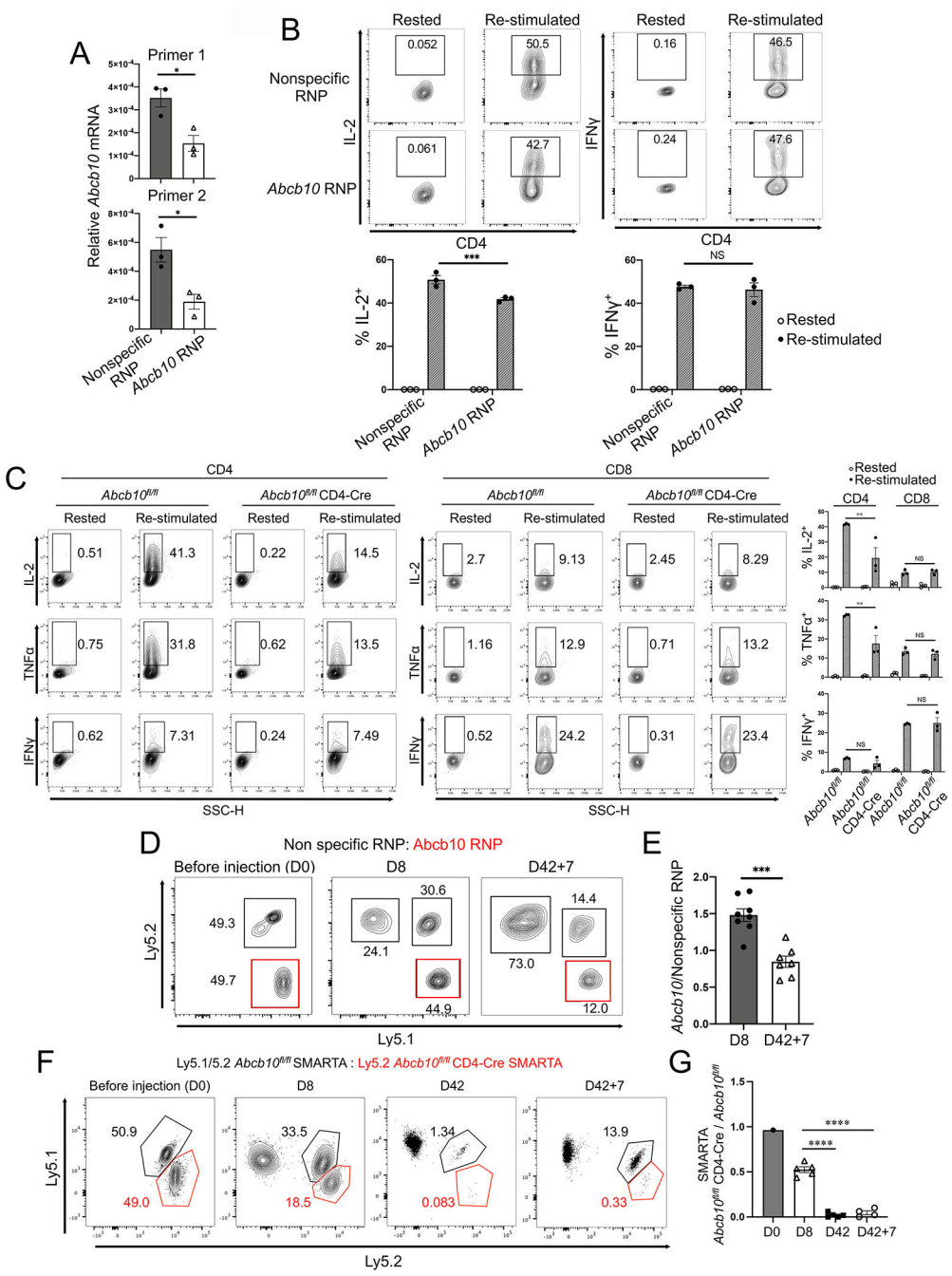

FIGURE 3.

Loss of Abcb10 affected IL-2 production after restimulation of previously activated primary CD4 T cells in vitro. **(A)** CD4 T cell purified from spleen of C57BL/6J were electroporated with Non-specific RNP or *Abcb10* CRISPR RNP and cells were sorted on ATTO550+ transfected cell on the following day. After 5 days of electroporation, total RNA was purified for the *Abcb10* qPCR using TaqMan primers. This experiment was repeated once with similar results. (n=3 biologic replicates). **(B)** Cells indicated in A were stimulated with anti-CD3/CD28 antibody for 2 days, cells washed with PBS and rested in culture medium

for 8 days (Rested) or restimulated with anti-CD3/CD28 antibodies overnight after resting (Restimulated). Immunofluorescent intracellularly staining for IL2 and IFNγ cytokines was performed and IL2+ and IFNγ+ cells were gated and cell percentages were summarized on the right. Each symbol represents a biological replicate (n=3). **(C)** Pan T cells were purified from spleens of *Abcb10*$^{fl/fl}$ and *Abcb10*$^{fl/fl}$ CD4-Cre mice and treated same as in B. IL-2, TNFα and IFNγ cytokines on CD4 and CD8 T cells were detected by flow. Each symbol represents a biological replicate (n=3). **(D)** CD4 T cells purified from spleens of Ly5.1/5.2 SMARTA mice and Ly5.1/5.1 SMARTA mice were electroporated with Non-specific RNP or *Abcb10* CRISPR RNP and live and ATTO550 positive cells were sorted and the congenic marker different CD4 T cells were mixed at a 1:1 ratio. Before transferring into C57BL/6J recipient mice, real cell ratio was measured with flow on day 0. On the second day after transferring the recipient mice were infected with LCMV Armstrong at $2X10^5$ pfu per mouse through ip injection. At day 8 peak response of LCMV infection and day 42 days rechallenge the mice with LM-GP61 for 7 days, congenic marker Ly5.1 and Ly5.2 were showed by flow on CD4 + T cells. **(E)** The bar graph showed the ratio of donor cells transfected with Abcb10 CRISPR RNP and non-specific CRISPR RNP. Each symbol represents one mouse. (n=7–8 biologic replicates). **(F)** CD4 T cells were purified from Ly5.1/5.2 *Abcb10*$^{fl/fl}$ SMARTA and Ly5.2 *Abcb1* $^{fl/fl}$ CD4-Cre SMARTA mice and mixed at a 1:1 ratio and transferred into B6 Ly5.1 recipient mice with 20K for each cell. Then the recipient mice were received LCMV infection and LM-GP61 re-challenge with the same method as in (D). **(G)** Bar graph of the ratio of donor SMARTA CD4 T cells. Each symbol represents one mouse. (n=4–5 biologic replicates).

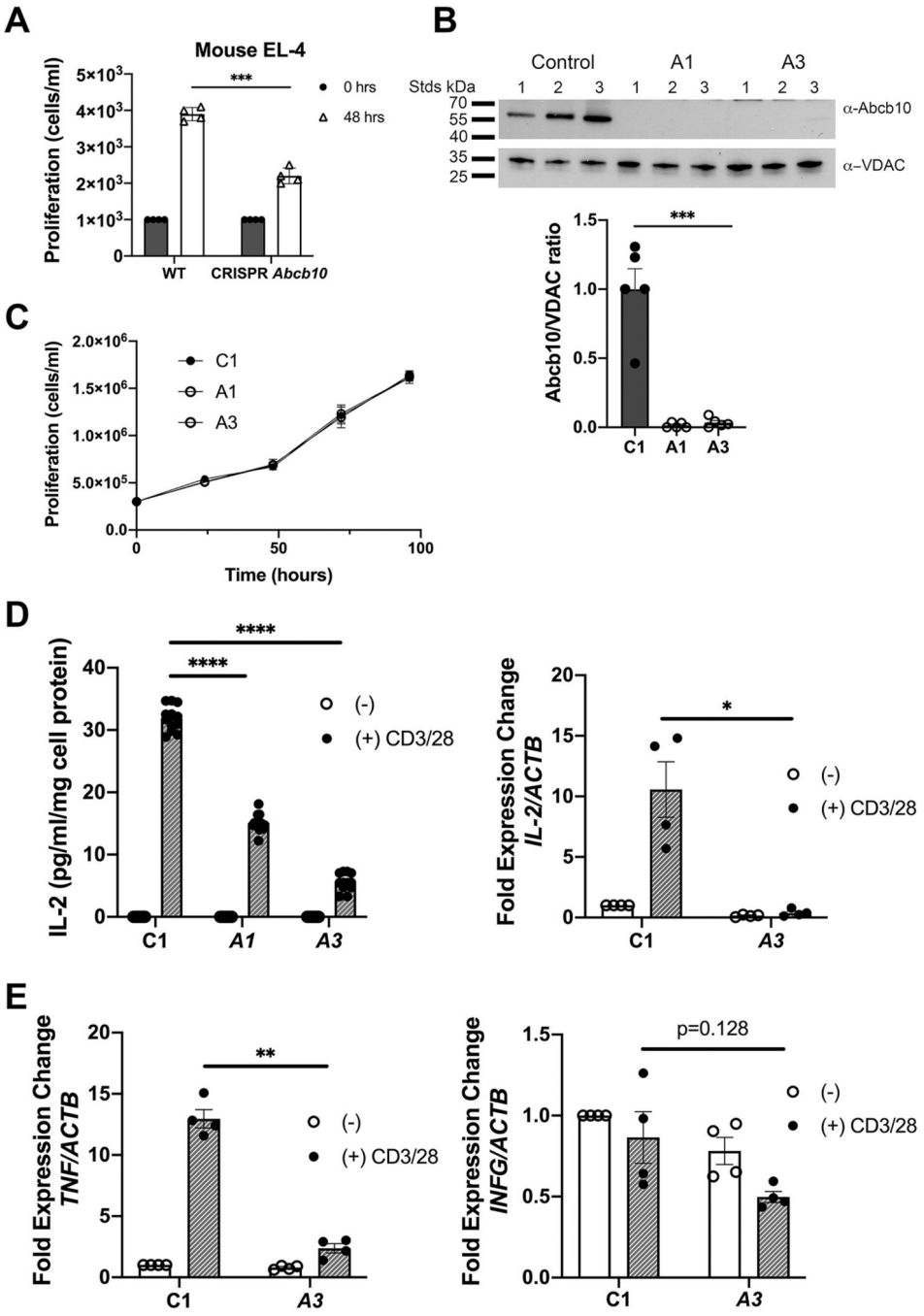

FIGURE 4.

Loss of Abcb10 in human Jurkat cells affected CD3/CD28-mediated activation. **(A)** EL4 mouse T cells were transduced with either control lentivirus (mCherry) or *Abcb10*-targeted CRISPR/Ca9 lentivirus (GFP). 48 hr post transfection cells were sorted by flow cytometry to obtain mCherry+ and GFP+ pools. Pools (1×10^3, time 0 hr) were grown in normal growth medium for 48 hr and proliferation assessed. Error bars represent SEM (n=4 biologic replicates). **(B)** Jurkat cells were transduced with either control lentivirus (mCherry) or *ABCB10*-targetted CRISPR/Cas9 lentivirus (Blue fluorescent protein (BFP)), cells sorted

for fluorescence and single cell seeded clones isolated and expanded. Mitochondria were purified from control cells (C1) and *ABCB10* mutants clones A1 and A3 and ABCB10 and VDAC levels measured by Western blot. A representative blot is shown of three biologic replicates. Western blots were quantified as describe in Materials and Methods. Error bars represent SEM. (n>4 biologic replicates). **(C)** Cell proliferation was determined for C1, A1 and A3 cell lines at 0–96 hr. (n≥4 biologic replicates). **(D)** C1, A1 and A3 were incubated with 25 μl/ml anti-CD3/CD28 for 72 hr (hatched bars) and IL-2 secretion measured by ELISA. (n=3 biologic replicates). RNA was isolated from four biologic replicates of C1 and A3 cells stimulated with CD3/CD28 for 72 hr and *IL-2* and *ACTB* transcripts determined using RT-qPCR. **(E).** Transcripts levels for *TNF*a and *INFG* were determined from samples as in D.

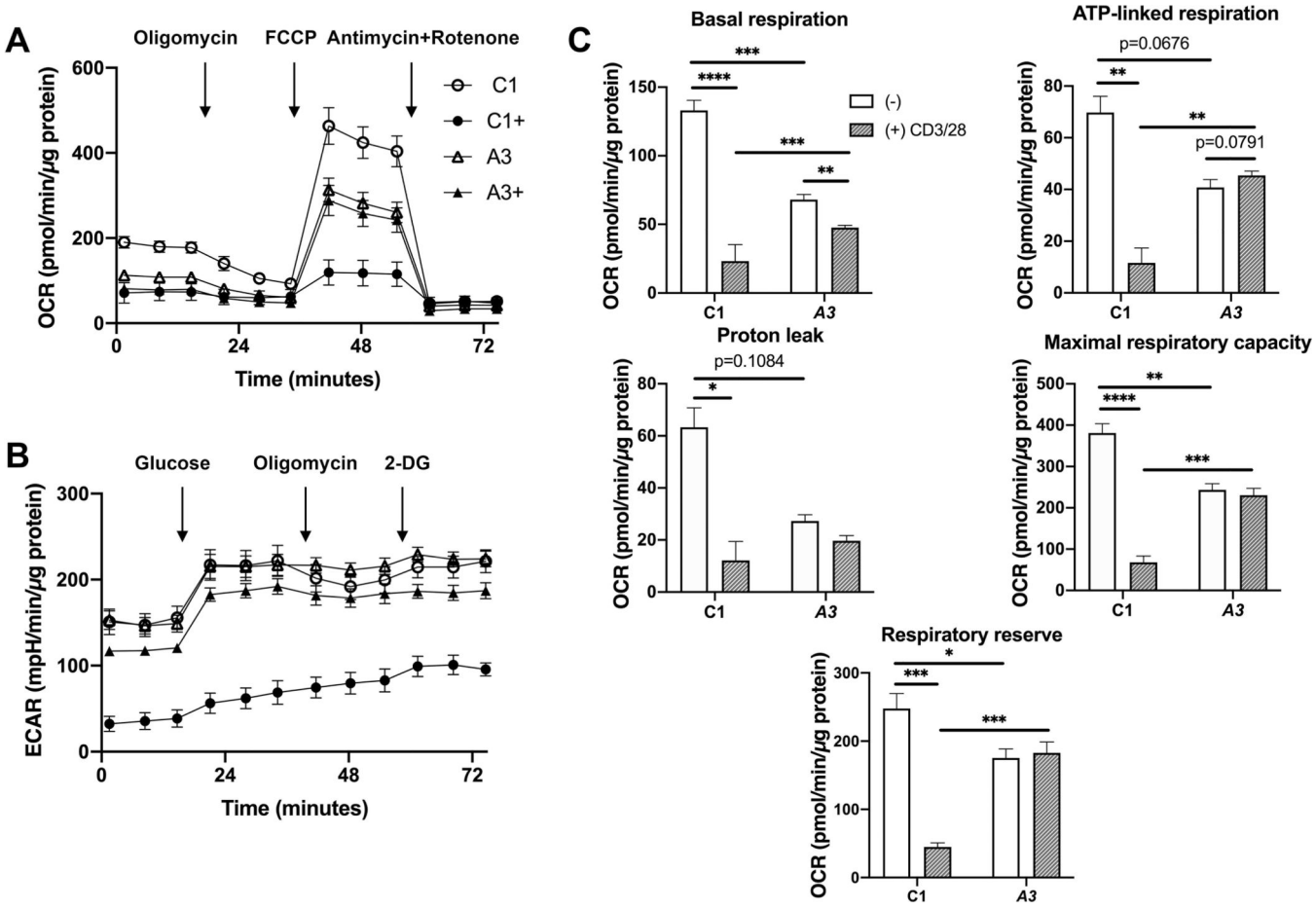

FIGURE 5.

Loss of ABCB10 resulted in altered metabolic activity in Jurkat cells. **(A)** Control C1 and *ABCB10* null A3 cells were incubated +/− anti-CD3/CD28 for 72 hr and then plated onto Seahorse 96 well plates precoated with CellTek (Corning). Cells were centrifuge onto plates at 1500 × g for 20 minutes and oxygen consumption (OCR) determined by Seahorse as described in Materials and Methods. **(B)** External acidification (ECAR) was determined on cells as in A. **(C)** Basal respiration, ATP-linked respiration, Proton leak, Maximal respiratory capacity and Respiratory reserve were determined as described (27). A representative analysis is shown. Error bars represent SEM of 12 biologic replicates.